



Formulation, Optimization and Evaluation of Eudragit RL 100 nanoparticles loaded with Quercetin for its Hypolipidemic action by using Animal Model

Virendra Singh¹, Mukul Singh², Mohammed Faisal Almutairi³, Abdullah Faisal Al-mutairi⁴, Nasser Faisal Alshahrani⁵, Mohammad Dabeer Ahmad⁶, Priya Pandey⁷, Md Salahuddin Ansari^{8*}

¹HR Institute of Pharmacy, 8th Km Stone, Delhi-Meerut Road, Merta, Ghaziabad-201003 (U.P).

²GNIT College of pharmacy, Plot No. 6-C, knowledge Park II, greater noida, Uttar Pradesh -201301.

³Prisons health Almalaz prison, Riyadh, Kingdom of Saudi Arabia.

⁴Aldwaa Pharmacy, king Abdullah Road, Unayzah, Kingdom of Saudi Arabia

⁵College of Pharmacy, Al-Dawadmi, Shaqra University, Saudi Arabia.

⁶Faculty of Pharmacy, Jahangirabad Institute of Technology, Jahangirabad, Barabanki, Uttar Pradesh – 225203 India.

⁷IIMT College of Pharmacy, Plot No. 19 & 20, Knowledge Park III, Greater Noida, Uttar Pradesh 201310.

^{8*}Department of Clinical Pharmacy, College of Pharmacy Al-Dawadmi, Shaqra University, Saudi Arabia.

***Corresponding author: - Md Salahuddin Ansari**

**Department of Clinical Pharmacy, College of Pharmacy Al-Dawadmi, Shaqra University, Saudi Arabia.*

E mail id: msalahuddin@su.edu.sa, Contact No: +966550094760

Article History	Abstract
<p>Received: Revised: Accepted</p>	<p>Quercetin, a potent pharmacological active phytochemical, plays a crucial role in drug therapy. However, its essential role is limited due to poor water solubility and low bioavailability. To overcome these limitations and enhance oral bioavailability, Quercetin loaded Eudragit nanoparticles were prepared using a single emulsification solvent evaporation method and optimized by applying Box-Behnken design. This study aimed to investigate the anti-hyperlipidemic potential of Quercetin in Triton WR-1339 induced hyperlipidemic rats. Hyperlipidemia was induced in rats using Triton WR-1339, and the hypolipidemic potential of Quercetin was evaluated at doses of 50 and 100 mg/kg. The results revealed that Quercetin significantly ($p \leq 0.005$) altered the serum levels of total cholesterol (TC), triglycerides (TG), low-density lipoprotein cholesterol, and high-density lipoprotein cholesterol, bringing them close to normal levels in Triton WR-1339 induced hyperlipidemic rats. Furthermore, both doses of Quercetin (50 and 100 mg/kg) showed significant reductions in TC and TG levels when compared to the standard atorvastatin treatment. The novel formulation of Quercetin loaded Eudragit polymeric nanoparticles displayed remarkable potential as a green antihyperlipidemic agent. These findings suggest that Quercetin loaded Eudragit nanoparticles can effectively mitigate hyperlipidemia and have the potential to be a promising therapeutic option for lipid disorders. The enhanced bioavailability and bioactivity of Quercetin delivered through this novel formulation open new possibilities for its clinical application in managing</p>

<p>CC License CC-BY-NC-SA 4.0</p>	<p>hyperlipidemia. Further research and clinical studies are warranted to explore its translational potential and wider applications in drug therapy.</p> <p>Keyword:- Quality by Design, Box-Behnken design, Nanoformulation, Hyperlipidemia, Eudragit RL100, Atorvastatin</p>
--	--

1. Introduction

In recent years, there has been a growing interest in the development of nanotechnology-based drug delivery systems to enhance the therapeutic efficacy of various bioactive compounds. Among these, polymeric nanoparticles have gained significant attention due to their unique properties, such as small size, high surface area-to-volume ratio, and controlled release capabilities. In particular, Eudragit RL 100, a biocompatible and biodegradable polymer, has shown great potential in the formulation of nanoparticles for drug delivery applications.

Quercetin, a natural flavonoid (1) compound found in various fruits and vegetables, has been recognized for its numerous health benefits, including antioxidant, anti-inflammatory, and anticancer properties. However, the clinical application of quercetin is often limited by its poor aqueous solubility and low bioavailability (2). To overcome these challenges, the encapsulation of quercetin into polymeric nanoparticles can provide an effective strategy for improving its stability, solubility, and targeted delivery to specific sites of action.

In this study, we aimed to develop and optimize quercetin-loaded Eudragit RL 100 polymeric nanoparticles as a potential drug delivery system. The formulation of these nanoparticles involved the preparation of Eudragit RL 100-based nanocarriers using various techniques such as solvent evaporation, emulsion-solvent evaporation, or nanoprecipitation. The optimization process was carried out to achieve desirable nanoparticle characteristics, including particle size, encapsulation efficiency, and drug release profile (3).

The characterization of the formulated nanoparticles was conducted using various *in vitro* techniques. Physicochemical properties such as particle size, morphology, and zeta potential were evaluated using dynamic light scattering and scanning electron microscopy. The drug encapsulation efficiency and drug release kinetics were assessed using validated analytical methods. Furthermore, *in vitro* studies were performed to evaluate the cytotoxicity and cellular uptake of the quercetin-loaded nanoparticles using relevant cell lines.

The results obtained from this study will provide valuable insights into the formulation, optimization, and *in vitro* characterization of quercetin-loaded Eudragit RL 100 polymeric nanoparticles. These findings may contribute to the development of a novel drug delivery system for enhanced therapeutic outcomes of quercetin in the treatment of hyperlipidemia (4), ultimately leading to its potential clinical applications in the field of medicine and healthcare.

2. Material and Methods

2.1 Materials

For the preparation and characterization of quercetin-loaded Eudragit RL 100 polymeric nanoparticles, various materials and reagents were employed. Quercetin, a natural flavonoid compound, was obtained from Sigma Aldrich, India. Eudragit RL 100, a biocompatible and biodegradable polymer suitable for nanoparticle formulation, was also procured from Sigma Aldrich, India. In addition to the specific components, other chemicals and solvents necessary for the experimental procedures were purchased from Fisher Scientific, Mumbai, India. Throughout the entire experimentation process, Water for Injection (WFI) was utilized as the solvent for preparing solutions and suspensions, ensuring the purity and quality of the samples.

Male Wistar albino rats weighing between 160 and 200 gm were used. The animals were obtained from a vendor registered with the Committee for the Purpose of Control and Supervision of Experiments on Animals (CCSEA). On April 10, 2017, the Institutional Animal Ethics Committee (IAEC/SHUATS/ PA/2017III/ SVKS02) approved the study, indicating that it complied with ethical standards and recommendations for the humane treatment of animals in research. The rats were kept in a polyacrylic cage with environmental conditions that comprised a humidity range of 60%-65% and a room temperature range of 24°C-27°C that mimicked natural light patterns.

2.2 Methods

2.2.1 Formulation of Quercetin loaded Eudragit RL 100 polymeric nanoparticles

Dissolution of Quercetin and Eudragit RL 100: Quercetin (1mg) and Eudragit RL 100 (5.16 mg) were accurately weighed and dissolved in acetone, forming the organic phase. The organic phase acts as the carrier for quercetin and the polymer, Eudragit RL 100. **Preparation of Aqueous Phase:** An aqueous solution of 4.5% w/v Polyvinyl alcohol (PVA) was prepared. PVA served as the aqueous phase for the emulsification process. **Emulsification:** The organic phase, containing quercetin and Eudragit RL 100, was added dropwise into the aqueous phase while continuously stirring the mixture. This step is crucial for forming the emulsion. **Homogenization:** The emulsion was further homogenized using an IKA high shear homogenizer at 16000 rpm for 10 minutes. The high shear forces during homogenization help in reducing the particle size and ensuring uniform distribution of the components. **Sonication:** The homogenized mixture was subjected to sonication using an Ultra Probe sonicator (UP50H, Hielscher) for 12 minutes. Sonication aids in breaking down larger aggregates and promotes the formation of stable nanoparticles. **Solvent Evaporation:** The sonicated emulsion was left to stir overnight on a magnetic stirrer (IKARH digital) at a speed of 500 rpm. This step allowed the organic solvent (acetone) to evaporate slowly, leaving behind the quercetinloaded Eudragit RL 100 nanoparticles. **Product Isolation:** Once the organic solvent was completely evaporated, the resulting nanoparticle product was obtained. To remove any residual solvent or unencapsulated quercetin, the product was subjected to centrifugation. **Lyophilization:** The centrifuged product was then subjected to lyophilization (freeze-drying) to convert the nanoparticles into a dry, stable powder form. Lyophilization helps to enhance the long-term stability of the nanoparticles. **Storage:** The lyophilized quercetinloaded Eudragit RL 100 nanoparticles were stored in airtight vials to ensure their integrity and prevent any degradation until further characterization and use(3, 5).

2.2.2 Risk assessment Studies

In the context of formulating Quercetin, the application of Quality by Design (QbD) principles can help ensure an efficient manufacturing process and reduce the risk of potential product failure. QbD involves a systematic approach that incorporates real-time scientific knowledge to design and develop a robust formulation. The first step in QbD is defining the Quality Target Product Profile (QTTP). This involves setting clear objectives for the desired characteristics and performance of the dosage form containing Quercetin. The QTTP serves as a reference point for all subsequent development and optimization activities. Critical Quality Attributes (CQAs) are then determined, which are the key attributes that directly impact the safety, efficacy, and quality of the formulated product(6). In the case of Quercetin, these CQAs may include parameters such as particle size, encapsulation efficiency (EE%), and zeta potential. Formulation investigations led to the selection of the experimental components that were dependent and independent, as shown by the **Ishikawa diagram**(Figure 1)(7).

Risk assessments play a crucial role in QbD, helping identify potential failure modes and associated risks during the formulation process. By conducting risk assessments, critical material attributes (CMAs) and critical process parameters (CPPs) can be identified(8).

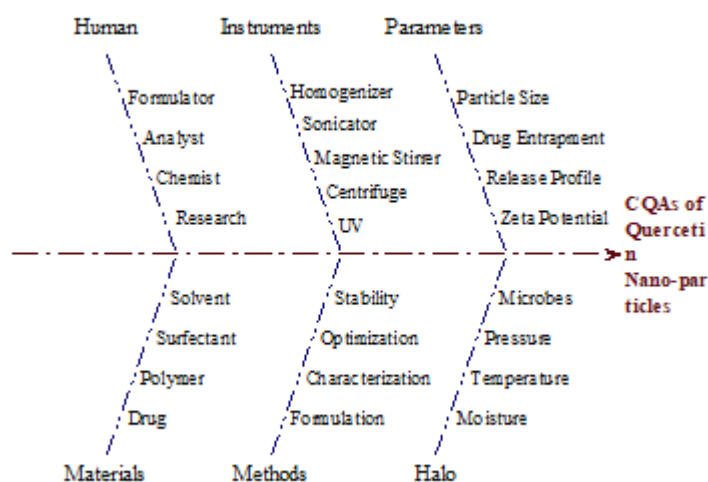


Figure 1: Ishikawa diagram

2.2.3 Factor Screening Design Studies

The design of experiments (DOE) is a systematic approach used to efficiently and effectively gather information and optimize processes(9). The DOE involves preliminary screening and surface response methodology (RSM), and the Plackett-Burman design (PBD) was employed for factor screening. Minitab™ 17 software was used to estimate the correlation between factors and responses(10).

Preliminary screening is the initial step in the DOE, where a large number of factors that could potentially influence the response are identified. These factors can be related to a manufacturing process, a chemical reaction, or any other system you are trying to optimize or improve(11). The objective of preliminary screening is to identify the most important factors that have a significant impact on the response. However, it is not designed to optimize the process but rather to select the most influential factors to be studied further. Once the significant factors are identified through the Plackett-Burman design, the next step is to optimize the process using the surface response methodology (RSM). RSM is a collection of statistical and mathematical techniques used to model the relationship between the response variable and the significant factors(12). The goal is to find the optimal conditions or settings for these factors that lead to the best possible response. RSM helps to construct a response surface, which is a mathematical model that predicts how the response variable behaves based on the levels of the significant factors. Minitab™ 17 was used to estimate the correlation between the factors identified through the Plackett-Burman design and the responses obtained from the surface response methodology. The software allows you to perform regression analysis to build the response surface models and assess the relationship between factors and responses.

2.2.4 Optimization and statistical analysis

The independent variables (factors) that significantly affect the answer have now been found. The concentration of the surfactant (A), polymer (B), homogenizer speed (C), and ultrasonication time (D) are these variables. We created a mathematical model to describe the link between the response and the independent variables (A, B, C, and D). Given that there are four elements, a quadratic equation that includes both linear and interaction terms is probably the best fit. Curvature and interaction effects can be accounted for using the quadratic model(13).

Using the experimental data from the PBD and possibly additional experiments. This model involved the main effects (A, B, C, D), interaction terms (AB, BC, AD, AC, BD, CD), and the quadratic terms (A², B², C², D²). The equation was:

$$\text{Response} = \beta_0 + \beta_1A + \beta_2B + \beta_3C + \beta_4D + \beta_{12}AB + \beta_{13}AC + \beta_{14}AD + \beta_{23}BC + \beta_{24}BD + \beta_{34}CD + \beta_{11}A^2 + \beta_{22}B^2 + \beta_{33}C^2 + \beta_{44}D^2 + \text{Error}$$

Where $\beta_0, \beta_1, \beta_2, \dots, \beta_{44}$ are the coefficients estimated from the data.

We projected the ideal values of the independent variables (A, B, C, and D) that will lead to the desired response using the fitted quadratic equation. For your particular response variable, this predicted formulation provides the circumstances that are anticipated to produce the greatest results.

The in-vitro characterization process used the expected formulation that was derived from the optimization step. In-vitro characterization entailed conducting studies or tests without using a living thing to evaluate the formulation's numerous qualities and features.

2.3Determination of Particle size, shape and surface

The particle size of Quercetin loaded Eudragit RL 100 nanoparticles is measured using two techniques: Zeta sizer and photon correlation spectroscopy. Both methods are based on the principle of light scattering. The Zeta sizer and photon correlation spectroscopy provide information about the average particle size and size distribution of the nanoparticles in a sample(14). Particle size is a critical factor in nanoparticle formulations, as it directly influences their stability and bioavailability(15). Optimal particle size is often desired to ensure uniformity and efficient delivery to the target site. Transmission electron microscopy (TEM) was employed to visualize the morphology of the Quercetin loaded Eudragit RL 100 nanoparticles. TEM offers higher resolution images that allow visualization of internal structures and finer details of the nanoparticles. The TEM helps in gaining a comprehensive understanding of the physical characteristics of the nanoparticles. Surface charge of the nanoparticles, also known as zeta potential(16), is determined using the dynamic scattering analyzer (Desla Nano C, Beckman Coulter, UK) in a polystyrene cuvette. Zeta potential is a measure of the electrical charge at the nanoparticle surface and provides valuable information about their stability and potential interactions with biological systems. Nanoparticles with appropriate surface charge properties are less likely to aggregate, which is essential for maintaining their stability in various applications, including drug delivery(17).

2.4Determination of entrapment efficiency

Entrapment efficiency is a measure of how much of the drug is successfully encapsulated within the nanoparticles during the drug loading process(18). A higher entrapment efficiency indicates a larger proportion of the drug is retained within the nanoparticles, which is desirable for efficient drug delivery(19). The method used to determine entrapment efficiency involves separating the nanoparticles from the free drug in the supernatant using centrifugation.

A known quantity of Quercetin loaded Eudragit RL 100 nanoparticles was suspended in acetone. Acetone was used to break down or disrupt the nanoparticle matrix and release the drug. The suspension of nanoparticles in acetone was subjected to centrifugation at 10,000 rpm for 10 minutes. Centrifugation was used to separate the nanoparticles from the acetone and the released or unencapsulated drug. After centrifugation, the supernatant containing the free drug was separated from the nanoparticles, which form a pellet at the bottom of the centrifuge tube. The supernatant was analyzed using a UV-visible spectrophotometer at the absorption band of 240–280 nm(20). Quercetin had characteristic absorbance in this wavelength range, allowing for its quantification. Entrapment efficiency was calculated based on the difference between the initial amount of drug used for loading and the amount of free drug detected in the supernatant after centrifugation.

$$\%EE = \frac{\text{Drug incorporated} - \text{free drug}}{\text{Drug incorporated}} * 100\%$$

2.5 In vitro drug release studies

The in-vitro drug release study of Quercetin from Quercetin loaded Eudragit RL 100 nanoparticles was conducted using the dialysis membrane (bag) method. This method allows for the controlled release of the drug from the nanoparticles into a surrounding medium, which in this case is pH 7.4 PBS saline. The drug release kinetics were evaluated using various mathematical models, including zero-order, first-order, Higuchi model, and Peppas-Korsmeyer model(21, 22).

An optimized volume of Quercetin loaded Eudragit RL 100 nanoparticles was taken and placed into a dialysis bag with a molecular cut-off of 12,000-14,000(23). A beaker containing 100 ml of pH 7.4 PBS saline was used as the release medium. The pH of 7.4 is designed to simulate the physiological conditions of the body and temperature of the release medium was maintained at $37^{\circ}\text{C} \pm 0.5^{\circ}\text{C}$. At specified time intervals (0.5, 1, 2, 4, 6, 8, 12, and 24 hours), aliquots of the release medium were collected to quantify the amount of Quercetin released. The samples were collected in triplicate to ensure accuracy and reproducibility (n=3). To maintain sink conditions, the same quantity of pH 7.4 PBS saline was supplemented into the release medium each time a sample was collected. The collected samples were analyzed using a UV-visible spectrophotometer at the absorption band of 240-280 nm.

To evaluate the best-fit model, the regression coefficient (R^2) values were compared. A value closer to 1 indicates a better fit of the model to the experimental data. The model with the highest R^2 value is considered the standard drug release kinetic data(24) for Quercetin loaded Eudragit RL 100 nanoparticles in the given experimental conditions.

2.6 Cytotoxicity

The MTT assay was used to investigate the cytotoxicity of Quercetin loaded Eudragit RL 100 nanoparticles on HeLa cell lines (Sigma Aldrich, India). The MTT assay is a widely used method for assessing cellular viability, and it is based on the reduction of the MTT reagent (Sigma Aldrich, India) to formazan crystals inside living cells. HeLa cell lines were seeded in 96-well plates at a density of 1×10^4 cells per well in 100 μL of growth medium. The cells were allowed to adhere and grow for 24 hours before the experiment. After 24 hours, the growth medium was removed, and the cells were exposed to various concentrations of Quercetin loaded Eudragit RL 100 nanoparticles aqueous dispersions. The nanoparticles were added to the cells in 100 μL of fresh medium. The cells were then incubated with the nanoparticles for an additional 24 hours under standard cell culture conditions (37°C , 5% CO_2). After the incubation with the nanoparticles, 20 μL of MTT stock solution (5 mg/mL in PBS) was added to each well. MTT is a yellow tetrazolium salt, and it is taken up by viable cells. The cells were further incubated for 4 hours at 37°C . During this time, viable cells metabolically reduce the MTT reagent to formazan crystals, which appear dark blue. After the 4-hour incubation, the medium was carefully removed from each well, and 150 μL of dimethyl sulfoxide (DMSO) was added to solubilize the formazan crystals. DMSO is used as it can dissolve the formazan crystals, producing a colored solution. The

absorbance of the colored solution was measured at 570 nm using an enzyme-linked immunosorbent assay (ELISA) reader(25). The absorbance at this wavelength is directly proportional to the number of viable cells in each well. The obtained absorbance data were averaged, and the percentage of cell viability was calculated using a standard equation. The experiments were performed three times, with each experiment conducted in triplicate. This provides multiple data points to ensure the reproducibility and reliability of the results.

$$\text{Cell Viability (\%)} = \frac{(\text{OD}_{\text{treatment}} - \text{OD}_{\text{medium}})}{(\text{OD}_{\text{control}} - \text{OD}_{\text{medium}})} \times 100$$

Where, OD= Optical density

2.7 Stability studies

To evaluate the product quality throughout time and in response to diverse environmental factors, the stability testing study for quercetinloaded Eudragit RL 100 nanoparticles was crucial. In order to assess the nanoparticles' long-term performance and shelf life, stability testing was performed under various storage circumstances, including temperature, humidity, and light. The formulations' freeze-dried powder was packed and sealed in amber-colored glass vials and placed in the stability chamber. According to the International Council for Harmonization of Technical Requirements for Pharmaceuticals for Human Use (ICH) recommendations, the stability chamber was adjusted at a temperature of 40°C and a relative humidity (RH) of 75°C(26).

Over the course of six months, the nanoparticles were tested for stability. Samples were periodically collected for analysis during this time. Particle size, zeta potential, and entrapment efficiency of quercetinloaded Eudragit RL 100 nanoparticles were examined.

2.8 Triton WR-1339 induced hyperlipidemia

The developed nanoformulation's antihyperlipidemic property was evaluated against an animal model of hyperlipidemia induced by Triton WR-1339 injections (200 mg/kg, intraperitoneal) in phosphate-buffered saline (pH 7.4). The animals were given free access to food and water throughout the experiment(27).

Five groups of six animals each were created by randomly dividing the animals. Rats in the control group (GP-I) were fed a typical pellet diet and given the treatment vehicle (distilled water). Triton WR-1339 (200 mg/kg, intraperitoneal) was administered to the hyperlipidemic control group (GP-II) in addition to vehicle. Triton WR-1339 (200 mg/kg, intraperitoneal) was administered to the GP-III and GP-IV (Quercetin-treated groups) and Quercetin (developed nanoformulation, 50 mg/kg and 100 mg/kg, p.o.) respectively. Atorvastatin (20 mg/kg, p.o.) and Triton WR-1339 (200 mg/kg, intraperitoneal) were administered to the control group (GP-V).

Blood samples were taken through retro-orbital sinus after the prescribed treatment period of 24 hours (28). Using a Beckman Coulter AU480 automated analyzer, the following parameters were measured: total cholesterol (TC), triglycerides (TG), high-density level cholesterol (HDL-C), low-density level cholesterol (LDL-C), and very low-density level cholesterol (VLDL-C).

3. Statistical analysis

The experimental data obtained from the study were expressed as Mean ± Standard error of the mean (SEM). Statistical analysis of the data was performed using analysis of variance (ANOVA). After ANOVA, the Dunnett test was used for post hoc analysis when necessary. The Dunnett test is a multiple comparison test that compares the mean of each group to a control group. GraphPad Prism 5, a popular software package, was used for statistical analysis and graph representation. p-value < 0.05 was considered statistically significant, indicating that there is less than a 5% chance of observing the results due to random variation alone. For formulation optimization, different software tools were used i.e. Minitab™ 17 (UK) was employed for primary factor screening and Design Expert 10 (MN, USA) was used for response surface methodology (RSM).

4. Result and Discussion

4.1 Box-Behnken Design

BBD is a response surface methodology used for optimizing processes and analyzing the interactions between multiple factors. Here, BBD was applied to optimize the formulation of a system with 4 factors, each having 3 levels (Table 1)(25). Additionally, 3 center points were included to help define the region of interest and provide replication for assessing experimental variability. BBD generated a total of 31 runs, each representing a unique combination of factor levels. The factors being studied were likely related to the formulation of the Quercetin loaded Eudragit RL 100 nanoparticles, such as the concentrations of polymers, surfactants, homogenizer speed, and ultrasonication time. After conducting the experiments, the data for particle size, entrapment efficiency, and zeta potential were analyzed using ANOVA at a 95% confidence interval. Using the significant factors identified from the ANOVA, a quadratic equation was generated using Minitab™ 17 software. The coefficients in the quadratic equation are denoted by positive and negative signs, representing their synergistic and antagonistic effects, respectively. The generated quadratic equation is used to create response surface plots and contour plots. These plots help visualize the correlations and interactions between the independent variables (factors) and the measured responses (particle size, entrapment efficiency, and zeta potential).

Table 1: Independent and dependent variables along with their levels in BBD

Independent Variables (Factors)	Levels		
	Low (-1)	Medium (0)	High (+1)
A. Polymer concentration	1	5.5	8
B. Surfactant concentration	1	2.5	6
C. Homogeniser speed (rpm)	15000	16500	18000
D. Ultra-Sonication time (min)	10	12.5	15
Dependent variable (response)			Constraint
R3= Entrapment efficiency (%)			Maximum
R1=Particle size (nm)			100-200
R2=Zeta potential (mV)			Maximum

Table 2 summarizes the results of the dependent variables (particle size, zeta potential, and entrapment efficiency) obtained from the optimized values of the independent variables. These optimized values were predicted using the quadratic equation generated through the BBD and RSM analysis. The table includes both the predicted values and the corresponding experimental findings for comparison. The independent variables polymer, surfactant, homogenizer speed, and ultrasonication time had respective expected values of 2.56 mg, 2.97 mg, 135000 rpm, and 15 min (Figure 2). The fact that the predicted values showed a satisfactory correlation and minimum bias with the experimental findings is an important finding. It indicates that the quadratic equation derived from the BBD accurately represents the relationship between the independent variables and the dependent variables (particle size, zeta potential, and entrapment efficiency). The good correlation between the predicted and experimental values suggests that the model generated through the BBD accurately reflects the behavior of the system and can be relied upon for further optimization and formulation studies. As a result of the satisfactory correlation between predicted and experimental values, the optimized formulation was selected for further studies. This means that the formulation with the specific set of optimized values for the independent variables (such as polymer concentration, surfactant concentration, homogenizer speed, and ultrasonication time) was found to have the desired characteristics in terms of particle size, zeta potential, and entrapment efficiency. The successful optimization of the formulation through the BBD and RSM analysis was a critical step in the development of an effective and reliable Quercetin loaded Eudragit RL 100 nanoparticle system. This formulation now used for further tested and evaluated in more comprehensive in vitro and in vivo studies to assess cytotoxicity and antihyperlipidemic profile.

Table 2: Optimized value of Independent Variables using BBD:

Independent Variables for response optimisation		
A.	Polymer (mg)	2.56
B.	Surfactant (mg)	2.97
C.	Homogeniser speed (rpm)	13500
D.	Ultra-Sonication time (min)	15
Optimised Result		
Dependent variable (response)	Predicted Value	Experimental Value*

R1=Particle size (nm)	154.66	183 ± 5.26
R2=Zeta potential (mV)	+17.09	+18 ± 2.13
R3= Entrapment efficiency (%)	71.92	69.87 ± 1.73

* Value expressed in Mean ± (SEM) (n=3)

Table 3: Statistical Analysis of Linear model:

Response	Linear model				
	F-Value	p-Value*	R-Sq (%)	Lack of fit	Remark
P. size	04.81	<0.05	81.26	0.651	Significant
% EE	14.31	<0.05	84.26	0.692	Significant
ZP (mV)	06.32	<0.05	87.72	0.316	Significant

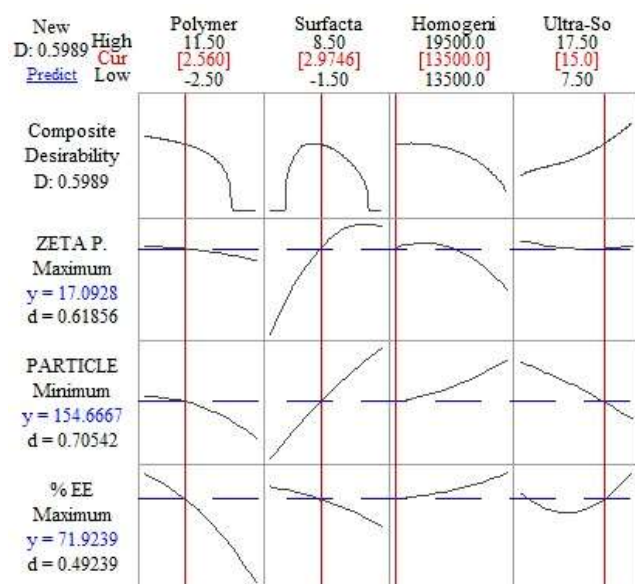


Figure 2: Optimization plot

Influence of independent variables on Particle size

Particle size is indeed a crucial factor in nanoparticle-based drug delivery systems, as it significantly influences various aspects of the formulation's behavior and performance(29). The quadratic model was used to study the relationship between the independent variables (such as polymer concentration and ultrasonication time) and the dependent variable (particle size) (30)in the Quercetin loaded Eudragit RL 100 nanoparticles.

The quadratic model used to predict particle size demonstrated statistical significance with a p-value < 0.05. A low p-value suggests that the model is highly significant, indicating that the independent variables have a significant effect on particle size. The F-value of 04.81 represents the goodness of fit of the model. The regression coefficient of 81.26% (Table 3) indicates the proportion of the total variation in particle size that can be explained by the model. A high regression coefficient suggests that the model provides a good representation of the relationship between the independent variables and particle size. The lack of fit test is used to assess whether the model adequately describes the experimental data. A lack of fit p-value greater than 0.05 (0.651 in this case) indicates that there is no significant lack of fit, meaning that the model adequately fits the experimental data. The results indicate that polymer concentration is the most influencing parameter on particle size. This means that changing the polymer concentration has a significant impact on the resulting particle size of the nanoparticles. On the other hand, ultrasonication time has an inverse relationship with particle size(31). An increase in ultrasonication time leads to the formation of smaller-sized particles due to the increased shear stress during the ultrasonication process.

Particle size was predicted to be 154.66 nm. This value was calculated, simulated, and derived from a theoretical model. Particle size was measured experimentally was 183 ± 5.26 nm, through the actual measurements and experiments (Figure 3).

Quadratic equation for particle size= $526 - 9.2 A + 30.2 B - 0.0316 C - 24.3 D - 0.154 A^2 - 0.201 B^2 + 0.000000 C^2 - 0.101 D^2 - 0.314 A^2B + 0.000833 A^2C - 0.114 A^2D - 0.001800 B^2C + 0.260 B^2D + 0.001667 C^2D$

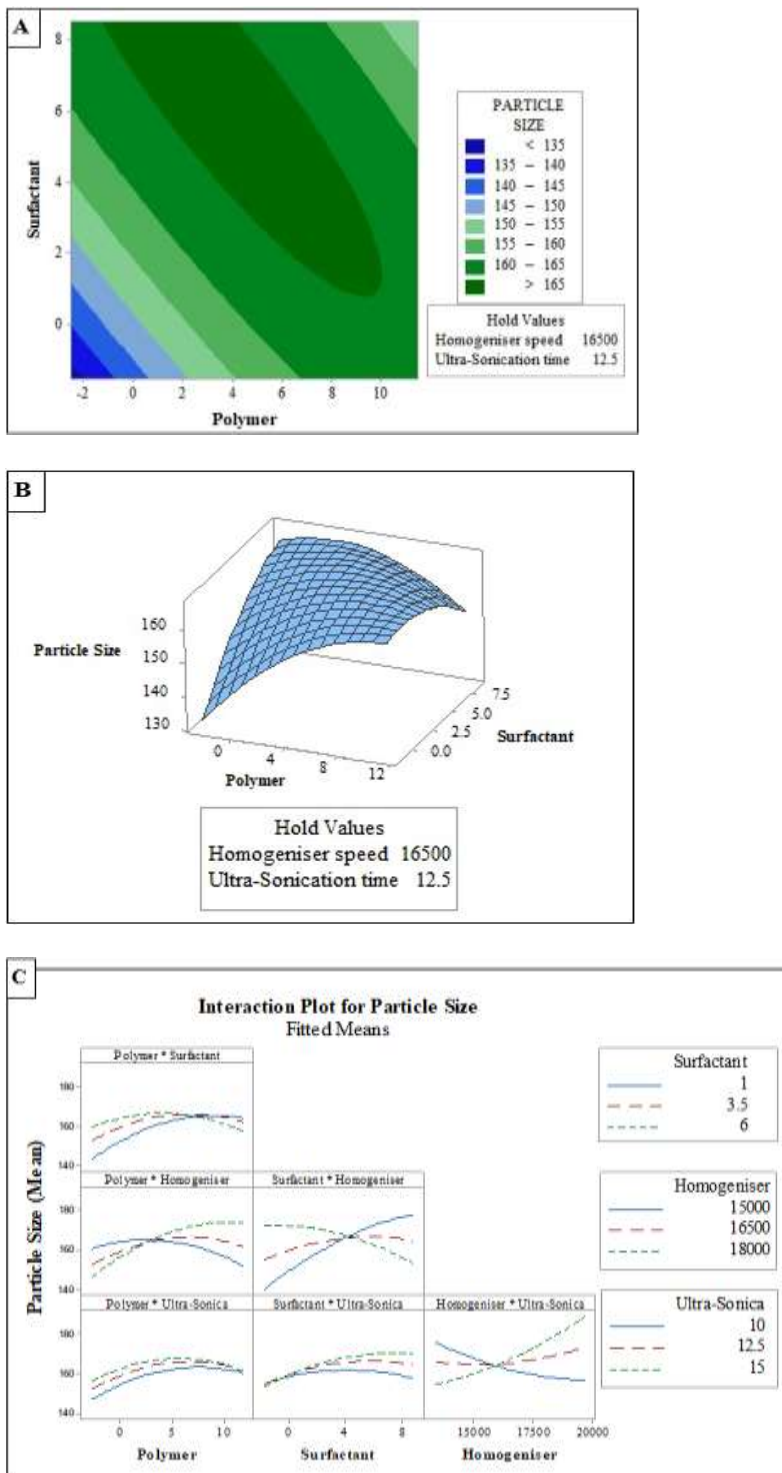


Figure 3: Effect of surfactant and polymer on Particle size A: Contour Plot, B: 3D Surface Plot, C: Interaction Plot

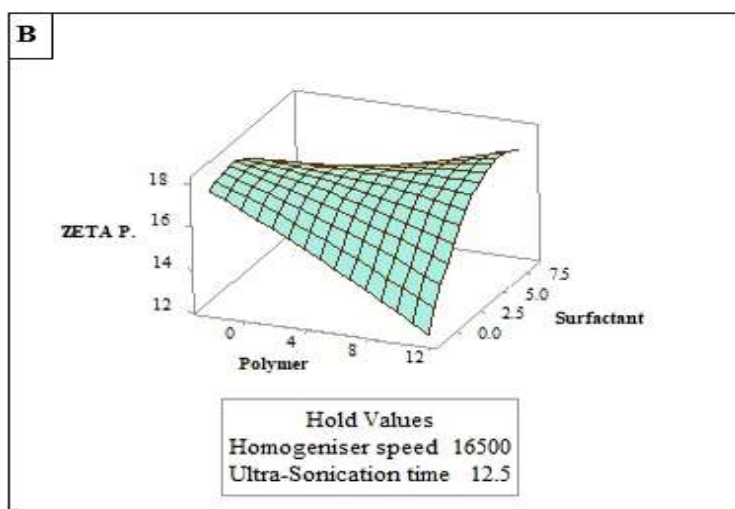
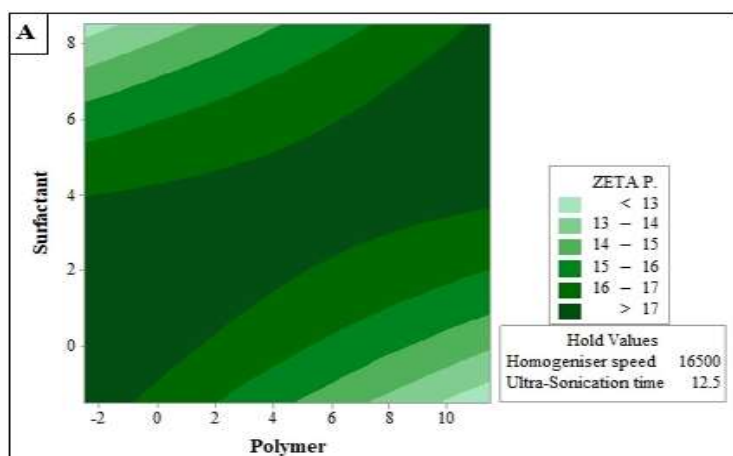
Influence of independent variables on Zeta potential

The polymeric nanoparticles (PNPs) showed a Zeta potential (ZP) ranging from +14 to +19 mV, indicating a confident level of variables and signifying a homogenous distribution. This homogenous distribution of Zeta potential ensures long-term stability of the nanoparticles, which is essential for their storage and potential application as drug delivery carriers(32).

The quadratic model used to predict Zeta potential showed statistical significance with an F-value of 06.32 and a p-value < 0.05. This indicates that the independent variables (such as polymer concentration, surfactant concentration, homogenizer speed, and ultrasonication time) collectively have a significant effect on the Zeta potential of the nanoparticles. The regression coefficient of 87.72 (Table 3) suggests that the model can explain approximately 87.72% of the total variation in the Zeta potential data. A high regression coefficient indicates that the model provides a good fit and accurately represents the relationship between the independent variables and Zeta potential under the specified experimental conditions. The lack of fit test is used to assess whether the model adequately describes the experimental data. In this case, the lack of fit p-value was 0.316(p>0.05), indicating the absence of significant lack of fit in the model. The results suggest that surfactant concentration has a significant impact on the Zeta potential of the nanoparticles. An increase in surfactant concentration led to a significant increment in the Zeta potential. This observation can be attributed to interfacial phenomena, where the surfactant molecules play a role in stabilizing the nanoparticles by forming a protective layer at the interface between the particles and the surrounding medium.

The Predicted value of Zeta potential was +17.09 mV while the experimental value was +18 ± 2.13 mV, indicating the precision and dependability of the adopted prediction model. This outcome exemplifies a sound prediction and offers useful information about the Zeta potential of the nanoformulation (Figure 4).

Quadratic equation for zeta potential = $-16.7 - 0.99 A + 0.75 B + 0.00485 C - 0.37 D - 0.0041 A^2 - 0.0881 B^2 - 0.000000 C^2 + 0.0119 D^2 + 0.0714 A*B + 0.000024 A*C + 0.0286 A*D - 0.000133 B*C + 0.1400 B*D - 0.000033 C*D$



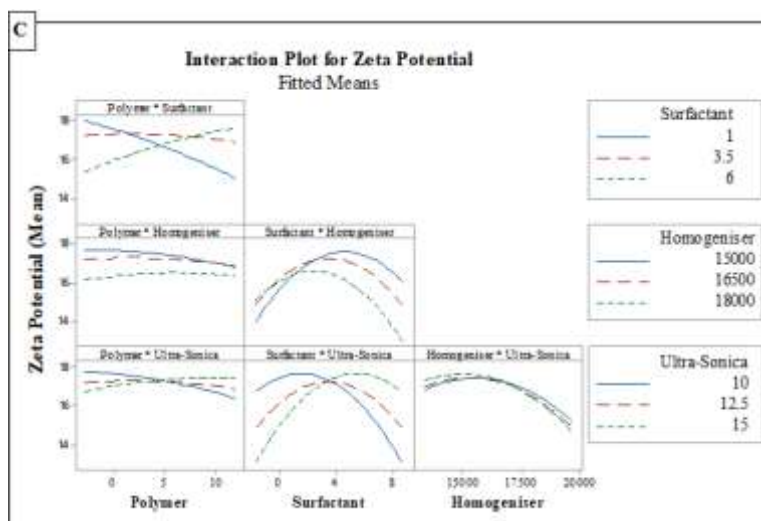


Figure 4: Effect of surfactant and polymer on %Zeta Potential A: Contour Plot, B: 3D Surface Plot, C: Interaction Plot

Influence of independent variables on entrapment efficiency

The entrapment efficiency of the Quercetin loaded Eudragit RL 100 nanoparticles varied between 67% to 77%. The F-value of 11.31 represents the goodness of fit of the model for entrapment efficiency. The regression coefficient of 84.26 (Table 3) indicates that the model can explain approximately 84.26% of the total variation in the entrapment efficiency data. A high regression coefficient suggests that the model provides a good representation of the relationship between the independent variables and entrapment efficiency and can accurately predict entrapment efficiency under the specified experimental conditions(33). A lack of fit p-value greater than 0.05 (0.692 in this case) indicates that there is no significant lack of fit in the model. This means that the model fits the experimental data well and is suitable for predicting entrapment efficiency. The results suggest that the Eudragit RL 100 polymer concentration has a positive influence on entrapment efficiency. As the concentration of Eudragit RL 100 RL100 polymer increases, the entrapment efficiency of the Quercetin loaded Eudragit RL 100 nanoparticles also increases. This indicates that higher concentrations of the polymer can enhance the entrapment of Quercetin in the nanoparticles, leading to a higher entrapment efficiency. The positive influence of Eudragit RL 100 RL100 polymer concentration on entrapment efficiency suggests that optimizing the polymer concentration could be a key factor in achieving higher entrapment efficiency and thereby improving the overall performance and effectiveness of the Quercetin loaded Eudragit RL 100 nanoparticles for drug delivery applications.

A theoretical model was used to calculate, simulate, and determine the estimated value (71.92%) of entrapment efficiency. While the experimental value of entrapment efficiency was 69.87 ± 1.73 %, through the actual measurements and experiments (Figure 5).

Quadratic equation for entrapment efficiency = $99.1 - 0.60 A - 0.51 B - 0.0021 C - 2.31 D - 0.0324 A^2 - 0.024 B^2 + 0.000000 C^2 + 0.116 D^2 + 0.021 A*B + 0.000155 A*C - 0.136 A*D + 0.000117 B*C - 0.090 B*D + 0.000017 C*D$

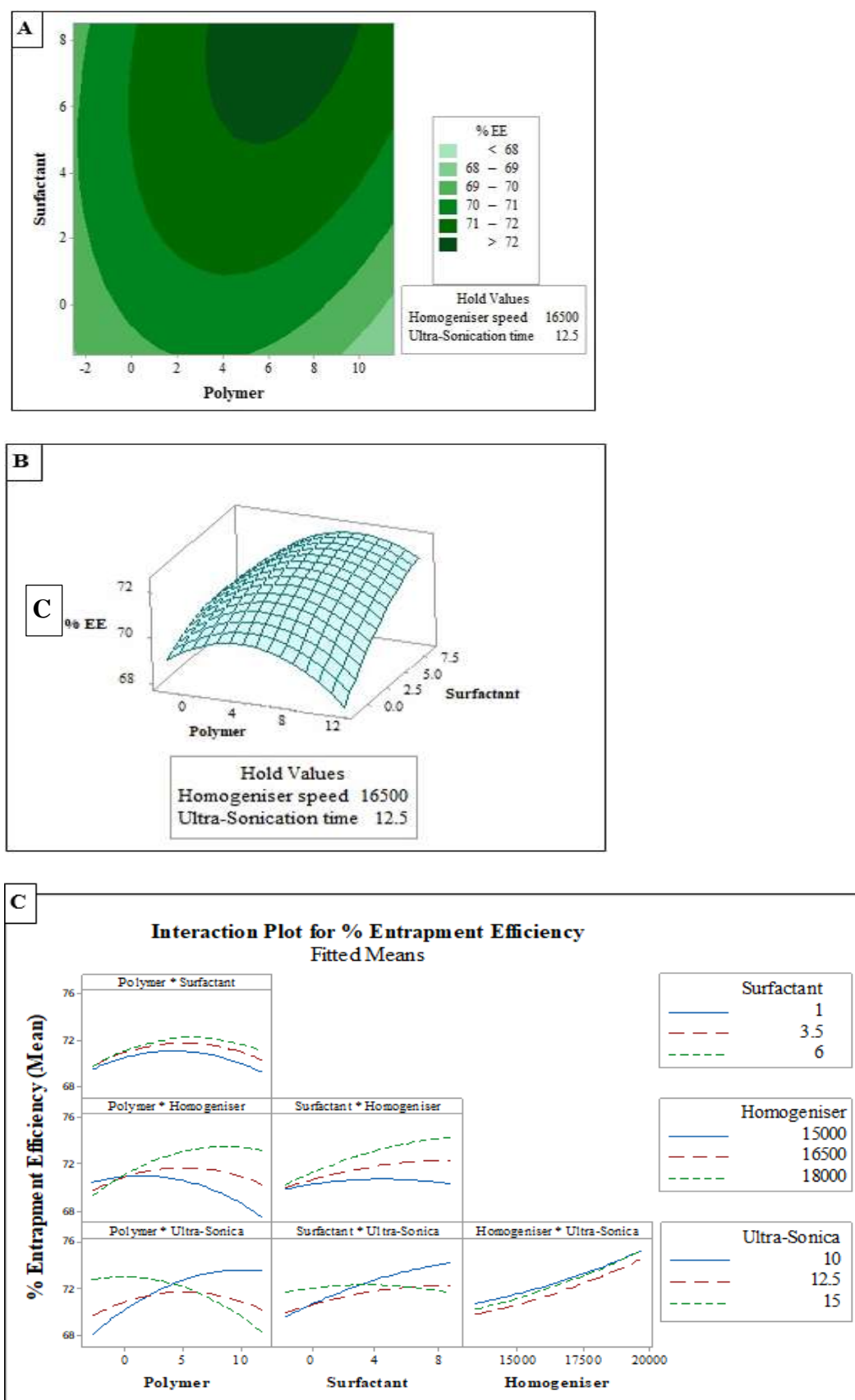


Figure 5: Effect of surfactant and polymer on %EE A: Contour Plot, B: 3D Surface Plot, C: Interaction Plot

4.2 Morphological study

The optimized nanoformulation was observed by using Transmission Electron Microscopy (TEM) (Technai-20G2, Philips). The purpose of TEM analysis is to visualize the individual particles in the formulation and obtain detailed information about their size, shape, and morphology. The optimized nanoformulation was

applied to a carbon-coated copper grid for TEM observation. This preparation method ensures that the nanoparticles are distributed evenly on the grid and allows for better imaging. The TEM images revealed that the individual particles in the optimized formulation were spherical in shape. The particle size range observed through TEM was between 142 to 185 nanometers (nm). The size range is crucial as it confirms that the nanoparticles fall within the desired range obtained from the previous analysis. The images showed that the particles in the optimized formulation appeared homogenous, meaning that they were similar in size and shape. Homogeneity is essential for consistent and reproducible drug delivery performance(34). The particles were observed to be discrete, indicating that they are separate entities and not aggregated or fused together. This is a favorable characteristic for nanoparticle-based drug delivery systems as it ensures uniform drug distribution and controlled drug release.

4.3 In vitro release of Quercetin

The in-vitro release rate of Quercetin loaded Eudragit RL 100 nanoformulation in a simulated biological environment (PBS at pH 7.4). The release profile was analyzed using a kinetic model, specifically the Peppas-Korsmeyer model. The regression coefficient, which is a statistical measure of how well the model fits the experimental data, was found to be 0.872 for the Peppas-Korsmeyer model(35). The Peppas-Korsmeyer model is considered more suitable than the Higuchi model for describing the release profile of Quercetin from the nanoformulation in this study (Figure 6). It suggests that the release of Quercetin from the nanoparticles follows a complex mechanism that is not solely based on diffusion through the matrix, as the Higuchi model assumes. The smaller particle size of the Quercetin loaded Eudragit RL 100 nanoparticles provided more surface area, facilitating the release of Quercetin from the formulation. This increased surface area allows for better interaction and movement of Quercetin across the gastrointestinal mucous membrane, potentially enhancing its absorption and availability for pharmacological action. Overall, the in-vitro release rate of Quercetin from the nanoformulation was found to be significant for its pharmacological action. This suggests that the formulated nanoparticles have the potential to deliver Quercetin effectively and efficiently, which can be advantageous for its therapeutic use in managing various medical conditions.

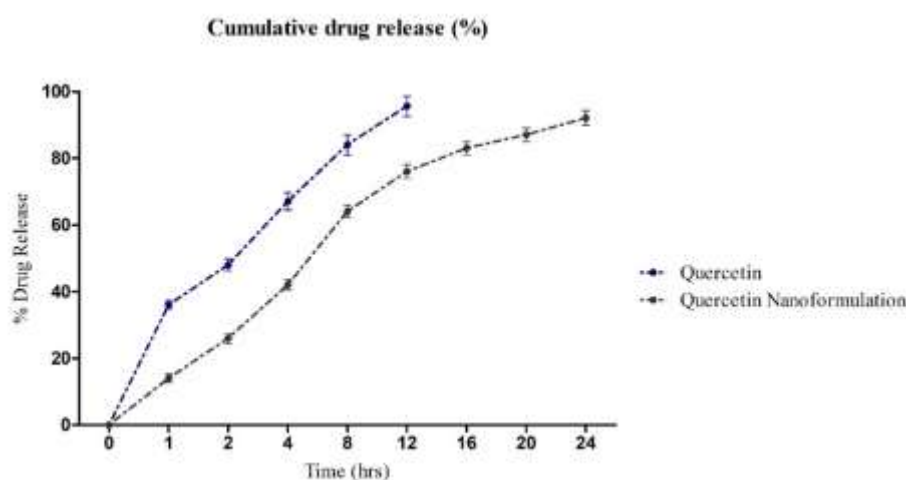


Figure 6: In-vitro release profile of QES-PN from nanoformulation in PBS (pH 7.4)

4.4 Cytotoxicity

The MTT assay was used to assess the cytotoxicity of Quercetin loaded Eudragit RL 100 nanoparticles on HeLa cells. The cells were treated with different concentrations of the nanoparticles ranging from 0.5 $\mu\text{g}/\text{mL}$ to 200 $\mu\text{g}/\text{mL}$ (36). The results of the MTT assay indicated that there was no statistically significant decrease ($P < 0.05$) in HeLa cell viability as the concentration of Quercetin loaded Eudragit RL 100 nanoparticles increased. This suggests that the nanoparticles, at different dilutions, did not have a significant negative impact on the viability of HeLa cells. A lack of statistically significant decrease in cell viability implies that the Quercetin loaded Eudragit RL 100 nanoparticles did not cause significant cell death or cytotoxicity within the concentration range tested. This finding is promising as it indicates that the nanoparticles may have good biocompatibility with HeLa cells and did not exert substantial toxic effects on the cells at the tested concentrations. It suggests that the nanoparticles could be considered as a safe carrier for delivering therapeutic agents like Quercetin to target cells without causing significant harm to healthy cells. The non-toxic nature of the nanoparticles at the tested concentrations opens up potential opportunities for their use in various

biomedical applications, particularly in drug delivery systems. It suggests that the nanoparticles could be considered as a safe carrier for delivering therapeutic agents like Quercetin to target cells without causing significant harm to healthy cells. Additional *in vitro* and *in vivo* studies, as well as detailed toxicity assessments, are essential to confirm the safety and efficacy of the Quercetin loaded Eudragit RL 100 nanoparticles for their intended applications.

4.5 Hypolipidemic activity

Triton WR-1339 causes acute hyperlipidemia by encouraging cholesterol production in the liver and blocking its excretion, delaying or preventing plasma clearance. After 24 hours of therapy, the levels of total cholesterol (TC), triglycerides (TG), HDL cholesterol (HDL-C), LDL cholesterol (LDL-C), and VLDL cholesterol (VLDL-C) were assessed in several experimental groups (Figure 7).

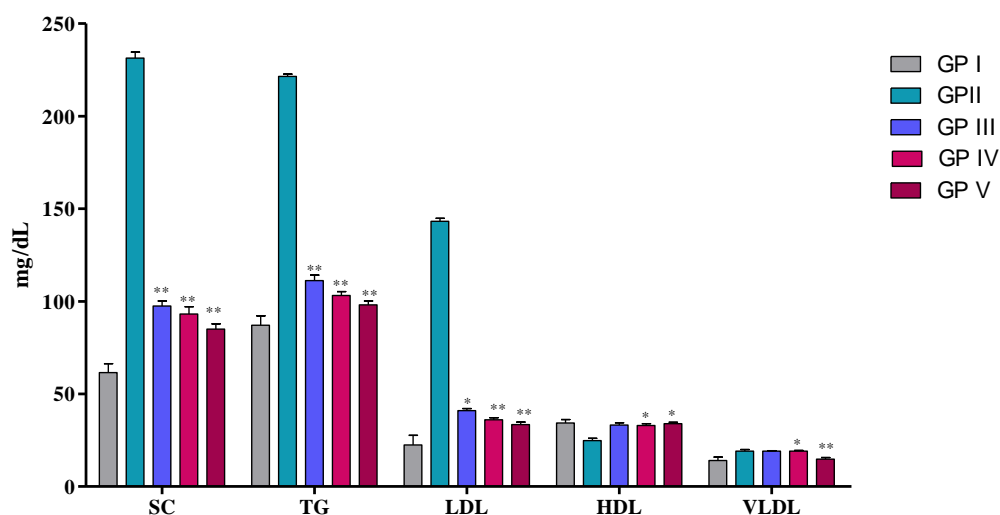


Figure 7: Effect of QES-PN on serum TC, TG, HDL-C, LDL-C, VLDL-C levels in Triton WR-1339 induced animal model (Values are expressed in Mean \pm SEM (n=6), $p \leq 0.05$, compared with hyperlipidemic control group (non-treated) with other treated groups)

The results indicate that treatment with Quercetin loaded Eudragit RL 100 nanoparticles (GP-III and GP-IV) and atorvastatin (GP-V) effectively reduced total cholesterol levels in hyperlipidemic animals compared to the hyperlipidemic control group (GP-II). The results showed that GP-I and GP-II had total cholesterol levels of 61.45 ± 4.89 mg/dL and 231.43 ± 3.12 mg/dL, respectively. The treated groups (GP-III to GP-IV) had total cholesterol levels that were, respectively, 97.45 ± 2.73 mg/dL, 93.16 ± 3.99 mg/dL, and 84.98 ± 2.91 mg/dL. These findings suggest that both Quercetin loaded Eudragit RL 100 nanoparticles groups may have potential therapeutic effects in reducing hyperlipidemia by lowering total cholesterol levels in the experimental animals. This indicates that these treatments might be beneficial in managing lipid metabolism and potentially lowering the risk of cardiovascular diseases associated with hyperlipidemia. However, these are experimental results confirmed the potential therapeutic effects of Quercetin loaded Eudragit RL 100 nanoparticles in reducing hyperlipidemia.

Triglyceride levels for GP-I and GP-II were 87.11 ± 5.01 mg/dL and 221.46 ± 1.32 mg/dL, respectively. The triglyceride levels in the treated groups (GP-III and GP-IV) with Quercetin loaded Eudragit RL 100 nanoparticles and the group (GP-V) treated with atorvastatin were significantly reduced compared to the hyperlipidemic control group. The triglyceride levels in these treated groups were found to be 111.21 ± 3.02 mg/dL, 103.12 ± 2.13 mg/dL, and 98.14 ± 2.11 mg/dL, respectively. These results further support the potential therapeutic effects of both Quercetin loaded Eudragit RL 100 nanoparticles groups in reducing hyperlipidemia by lowering triglyceride levels in the experimental animals. Lowering triglyceride levels can indeed be beneficial in managing lipid metabolism and reducing the risk of cardiovascular diseases associated with hyperlipidemia.

LDL-cholesterol is often referred to as "bad cholesterol" because high levels of LDL-cholesterol are associated with an increased risk of atherosclerosis and cardiovascular diseases. The LDL-cholesterol level in the normal

control group (GP-I) was 22.45 ± 5.14 mg/dL, while in the hyperlipidemic control group (GP-II), it was increased to 143.23 ± 1.67 mg/dL. This increase in LDL-cholesterol in the hyperlipidemic control group indicates successful induction of hyperlipidemia. As for the treated groups (GP-III and GP-IV) with Quercetin loaded Eudragit RL 100 nanoparticles and the group (GP-V) treated with atorvastatin, the data provided earlier showed a significant reduction in LDL-cholesterol levels compared to the hyperlipidemic control group. The LDL-cholesterol levels in these treated groups were reported to be 41.01 ± 1.06 mg/dL, 36.01 ± 1.12 mg/dL, and 33.44 ± 1.41 mg/dL, respectively. These results suggest that both Quercetin loaded Eudragit RL 100 nanoparticles and atorvastatin treatments have potential therapeutic effects in reducing LDL-cholesterol levels in hyperlipidemic animals. This reduction in LDL-cholesterol levels is beneficial for managing lipid metabolism and potentially lowering the risk of cardiovascular diseases associated with hyperlipidemia.

The VLDL-cholesterol level in the normal control group (GP-I) was 13.14 ± 0.89 mg/dL, while in the hyperlipidemic control group (GP-II), it was significantly increased to 19.37 ± 1.82 mg/dL. This significant increase in VLDL-cholesterol in the hyperlipidemic control group indicates successful induction of hyperlipidemia. VLDL-cholesterol is a type of lipoprotein that is primarily responsible for transporting triglycerides from the liver to peripheral tissues. Elevated VLDL-cholesterol levels are associated with increased cardiovascular risk. The results show that treatment with Quercetin loaded Eudragit RL 100 nanoparticles and atorvastatin led to a significant reduction in VLDL-cholesterol levels in the treated groups (GP-III, GP-IV, and GP-V) compared to the hyperlipidemic control group (GP-II). The VLDL-cholesterol levels in these treated groups were found to be 18.17 ± 0.89 mg/dL, 17.81 ± 0.26 mg/dL, and 15.21 ± 0.36 mg/dL, respectively. These findings suggest that both Quercetin loaded Eudragit RL 100 nanoparticles groups may have potential therapeutic effects in reducing VLDL-cholesterol levels in hyperlipidemic animals. Lowering VLDL-cholesterol can be beneficial in managing lipid metabolism and reducing the risk of cardiovascular diseases associated with hyperlipidemia.

High-density lipoprotein (HDL) cholesterol levels were 34.33 ± 1.87 mg/dL in GP-I and 24.78 ± 1.23 mg/dL in GP-II. The HDL-cholesterol levels in the treated groups (GP-III and GP-IV) with Quercetin loaded Eudragit RL 100 nanoparticles and the group (GP-V) treated with atorvastatin were significantly improved compared to the hyperlipidemic control group. The HDL-cholesterol levels in these treated groups were found to be 33.14 ± 1.31 , 32.99 ± 0.92 and, 33.89 ± 0.83 mg/dL, respectively. These results further support the potential therapeutic effects of both Quercetin loaded Eudragit RL 100 nanoparticles and atorvastatin in increasing HDL-cholesterol levels in hyperlipidemic animals. As mentioned earlier, HDL-cholesterol is considered "good cholesterol" because it plays a critical role in removing excess cholesterol from the bloodstream and transporting it to the liver for excretion, which can help reduce the risk of cardiovascular diseases. The findings indicate that the treatments might have a positive impact on HDL-cholesterol levels, which is beneficial for managing lipid metabolism and cardiovascular health in hyperlipidemic conditions.

Overall, the possibility that both Quercetinloaded Eudragit RL 100 nanoparticles and atorvastatin treatments may have a positive effect on the lipid profile, including lowering Quercetin levels of LDL cholesterol, VLDL cholesterol, triglycerides, and total cholesterol while raising levels of HDL cholesterol in hyperlipidemic animals(37, 38).

4.6 Stability Studies

As per the ICH guideline Q1A (R2), accelerated stability studies were conducted over a period of 6 months at $40 \pm 2^\circ\text{C}$, $75 \pm 5\%$ RH [Guideline, 2003] to assess the stability (39)of the Quercetin loaded Eudragit RL 100 nanoparticles. During the 6-month storage period, some changes in the physical characteristics of the nanoparticles were observed (Table 4). The particle size of the nanoparticles increased marginally from 183 ± 5.26 nm to 196 ± 4.01 nm over the 6-month storage. This increase in particle size suggests that there might have been some aggregation or agglomeration of the nanoparticles during the storage period. It is not uncommon for nanoparticles to undergo slight changes in size over time, especially under accelerated storage conditions. The entrapment efficiency of the nanoparticles decreased from $69.87 \pm 1.73\%$ to $67 \pm 1.67\%$ during the 6-month storage. A decrease in entrapment efficiency may indicate that some of the drug (Quercetin) was released from the nanoparticles over time, possibly due to changes in the nanoparticle structure or stability. The zeta potential of the nanoparticles also decreased from $+18 \pm 2.13\text{mV}$ to $+17 \pm 1.02\text{mV}$ during the storage period (Table 4). A decrease in zeta potential may be attributed to changes in the surface charge of the nanoparticles, which could influence their stability and interaction with the surrounding environment.

Despite the observed changes in particle size, entrapment efficiency, and zeta potential, the findings were statistically significant ($p < 0.05$), indicating that the prepared batches of the nanoformulation remained stable throughout the 6-month storage period. While there were some changes in the nanoparticle characteristics, these changes did not compromise the overall stability of the formulation. It is important that accelerated stability studies are conducted under more severe conditions than long-term stability studies, and the results obtained from accelerated studies provide valuable information about the potential stability issues that may arise in the formulation (40, 41). Further long-term stability studies under more moderate storage conditions would be necessary to confirm the stability of the Quercetin loaded Eudragit RL 100 nanoparticles over an extended period.

Table 4: Stability profile for particle size, zeta potential and % entrapment efficiency for 90 days storage period

Months	%EE	ZP	PS
0	69.87 ± 1.73	+18 ± 2.13	183 ± 5.26
1	69 ± 1.11	+18 ± 1.61	188 ± 2.31
3	68 ± 1.74	+18 ± 2.91	191 ± 3.79
6	67 ± 1.67	+17 ± 1.02	196 ± 4.01

(Mean ± SEM)

5. Conclusion

The present study marks a significant advancement in the field of hyperlipidemia treatment through the successful development and optimization of a nanoformulation containing Quercetin. The characterization of Quercetin loaded Eudragit polymeric nanoparticles has revealed their impressive lipid-lowering potential, as evidenced by the reduction in TC, TG, LDL-C, VLDL-C, and the increase in HDL-C levels in Triton WR-1339 induced hyperlipidemic rats. The rapid response observed within just 24 hours of treatment with the nanoformulation is particularly noteworthy, as it led to the normalization of plasma lipid levels in both nanoformulation-treated groups. This indicates the formulation's effectiveness in addressing hyperlipidemia and its potential to be a promising therapeutic option for managing lipid disorders. The study also highlights the importance of dosage optimization, with GP-IV, administered at a higher dose of 100 mg/kg, yielding more encouraging results than GP-III at 50 mg/kg. This finding underscores the relevance of exploring higher dosages to enhance the efficacy of the nanoformulation in combating hyperlipidemia. Overall, the findings of this research have substantial clinical significance and open up promising avenues for the treatment of hyperlipidemia using Quercetin loaded Eudragit polymeric nanoparticles. The ability to rapidly and effectively modulate lipid levels presents a potential alternative or complementary approach to current therapies, offering hope for improved outcomes in managing lipid disorders.

6. Conflict of Interest

By stating that there is no conflict of interest, the authors are assuring readers that their work is impartial and not influenced by any external factors that could undermine the study's integrity or validity. Such transparency is essential in maintaining the credibility and trustworthiness of scientific publications.

7. Acknowledgments:

The authors would like to thank the Deanship of Scientific Research at Shaqra University for supporting this work.

8. Funding:

The authors did not receive any funding.

9. References:

1. Wu T-H, Yen F-L, Lin L-T, Tsai T-R, Lin C-C, Cham T-M. Preparation, physicochemical characterization, and antioxidant effects of quercetin nanoparticles. *International journal of pharmaceutics*. 2008;346(1-2):160-8.

2. Tran TH, Guo Y, Song D, Bruno RS, Lu X. Quercetin-containing self-nanoemulsifying drug delivery system for improving oral bioavailability. *Journal of pharmaceutical sciences*. 2014;103(3):840-52.
3. Singh V, Pandey H, Misra V, Tiwari V, Srivastava P, Singh D. Hypolipidemic effect of [6]-Gingerol-loaded Eudragit polymeric nanoparticles in high-fat diet-induced rats and Gamma scintigraphy evaluation of gastric-retention time. *Journal of Applied Pharmaceutical Science*. 2022;12(6):156-63.
4. Wang T, Liu L, Deng J, Jiang Y, Yan X, Liu W. Analysis of the mechanism of action of quercetin in the treatment of hyperlipidemia based on metabolomics and intestinal flora. *Food & function*. 2023;14(4):2112-27.
5. Pool H, Quintanar D, Figueroa JdD, H. Bechara JE, McClements DJ, Mendoza S. Polymeric nanoparticles as oral delivery systems for encapsulation and release of polyphenolic compounds: impact on quercetin antioxidant activity & bioaccessibility. *Food Biophysics*. 2012;7:276-88.
6. Jankovic A, Chaudhary G, Goia F. Designing the design of experiments (DOE)—An investigation on the influence of different factorial designs on the characterization of complex systems. *Energy and Buildings*. 2021;250:111298.
7. Wong KC, Woo KZ, Woo KH. Ishikawa diagram. *Quality Improvement in Behavioral Health*. 2016:119-32.
8. Vanaja K, Shobha Rani R. Design of experiments: concept and applications of Plackett Burman design. *Clinical research and regulatory affairs*. 2007;24(1):1-23.
9. Ranga S, Jaimini M, Sharma SK, Chauhan BS, Kumar A. A review on Design of Experiments (DOE). *Int J Pharm Chem Sci*. 2014;3(1):216-24.
10. Vardhan H, Mittal P, Adena SKR, Mishra B. Long-circulating polyhydroxybutyrate-co-hydroxyvalerate nanoparticles for tumor targeted docetaxel delivery: Formulation, optimization and in vitro characterization. *European journal of pharmaceutical sciences*. 2017;99:85-94.
11. Lee E, Shah D, Porteus M, Wright JF, Bacchetta R. Design of experiments as a decision tool for cell therapy manufacturing. *Cytotherapy*. 2022;24(6):590-6.
12. Bezerra MA, Santelli RE, Oliveira EP, Villar LS, Escalera LA. Response surface methodology (RSM) as a tool for optimization in analytical chemistry. *Talanta*. 2008;76(5):965-77.
13. Anderson MJ, Whitcomb PJ. *RSM simplified: optimizing processes using response surface methods for design of experiments*: Productivity press; 2016.
14. Tscharnuter W. Photon correlation spectroscopy in particle sizing. *Encyclopedia of analytical chemistry*. 2000:5469-85.
15. Harde H, Das M, Jain S. Solid lipid nanoparticles: an oral bioavailability enhancer vehicle. *Expert opinion on drug delivery*. 2011;8(11):1407-24.
16. Clogston JD, Patri AK. Zeta potential measurement. *Characterization of nanoparticles intended for drug delivery*. 2011:63-70.
17. Sirisha V, D'Souza JS. Polysaccharide-based nanoparticles as drug delivery systems. *Marine OMICS*. 2016:663-702.
18. Mu L, Feng S-S. PLGA/TPGS nanoparticles for controlled release of paclitaxel: effects of the emulsifier and drug loading ratio. *Pharmaceutical research*. 2003;20:1864-72.
19. Das S, Chaudhury A. Recent advances in lipid nanoparticle formulations with solid matrix for oral drug delivery. *AAPS PharmSciTech*. 2011;12:62-76.
20. ur Rehman J, Ali I, Saifullah S, Ullah S, Imran M, Shah MR. Synthesis of quercetin based self-assembling supramolecular amphiphiles for amphotericin B delivery. *Journal of Molecular Liquids*. 2021;333:115941.
21. Costa P. An alternative method to the evaluation of similarity factor in dissolution testing. *International journal of pharmaceutics*. 2001;220(1-2):77-83.
22. Laracunte M-L, Marina HY, McHugh KJ. Zero-order drug delivery: State of the art and future prospects. *Journal of Controlled Release*. 2020;327:834-56.
23. Huang J, Wang Q, Chu L, Xia Q. Liposome-chitosan hydrogel bead delivery system for the encapsulation of linseed oil and quercetin: Preparation and in vitro characterization studies. *Lwt*. 2020;117:108615.
24. Gouda R, Baishya H, Qing Z. Application of mathematical models in drug release kinetics of carbidopa and levodopa ER tablets. *J Dev Drugs*. 2017;6(02):1-8.
25. Ni S, Hu C, Sun R, Zhao G, Xia Q. Nanoemulsions-based delivery systems for encapsulation of quercetin: Preparation, characterization, and cytotoxicity studies. *Journal of Food Process Engineering*. 2017;40(2):e12374.
26. Waterman KC, Carella AJ, Gumkowski MJ, Lukulay P, MacDonald BC, Roy MC, et al. Improved protocol and data analysis for accelerated shelf-life estimation of solid dosage forms. *Pharmaceutical research*. 2007;24:780-90.

27. Irudayaraj SS, Sunil C, Duraipandiyar V, Ignacimuthu S. In vitro antioxidant and antihyperlipidemic activities of *Toddalia asiatica* (L) Lam. leaves in Triton WR-1339 and high fat diet induced hyperlipidemic rats. *Food and chemical toxicology*. 2013;60:135-40.
28. Sikarwar MS, Patil M. Antihyperlipidemic activity of *Salacia chinensis* root extracts in triton-induced and atherogenic diet-induced hyperlipidemic rats. *Indian journal of pharmacology*. 2012;44(1):88.
29. Rampado R, Peer D. Design of experiments in the optimization of nanoparticle-based drug delivery systems. *Journal of Controlled Release*. 2023;358:398-419.
30. Venugopal V, Kumar KJ, Muralidharan S, Parasuraman S, Raj PV, Kumar KV. Optimization and in-vivo evaluation of isradipine nanoparticles using Box-Behnken design surface response methodology. *OpenNano*. 2016;1:1-15.
31. Fujimoto T, Terauchi S-y, Umehara H, Kojima I, Henderson W. Sonochemical preparation of single-dispersion metal nanoparticles from metal salts. *Chemistry of Materials*. 2001;13(3):1057-60.
32. Rahman HS, Rasedee A, How CW, Abdul AB, Zeenathul NA, Othman HH, et al. Zerumbone-loaded nanostructured lipid carriers: preparation, characterization, and antileukemic effect. *International Journal of Nanomedicine*. 2013:2769-81.
33. Tefas LR, Tomuța I, Achim M, Vlase L. Development and optimization of quercetin-loaded PLGA nanoparticles by experimental design. *Clujul Medical*. 2015;88(2):214.
34. Thabet Y, Elsabahy M, Eissa NG. Methods for preparation of niosomes: A focus on thin-film hydration method. *Methods*. 2022;199:9-15.
35. Hao J, Fang X, Zhou Y, Wang J, Guo F, Li F, et al. Development and optimization of solid lipid nanoparticle formulation for ophthalmic delivery of chloramphenicol using a Box-Behnken design. *International journal of nanomedicine*. 2011:683-92.
36. Zuleger S, Lippold BC. Polymer particle erosion controlling drug release. I. Factors influencing drug release and characterization of the release mechanism. *International journal of pharmaceutics*. 2001;217(1-2):139-52.
37. JuŸwiak S, Wójcicki J, Mokrzycki K, Marchlewicz M, Białeczka M, Wenda-Rózewicka L, et al. Effect of quercetin on experimental hyperlipidemia and atherosclerosis in rabbits. *Pharmacol Rep*. 2005;57(57):604-9.
38. Sahebkar A. Effects of quercetin supplementation on lipid profile: A systematic review and meta-analysis of randomized controlled trials. *Critical reviews in food science and nutrition*. 2017;57(4):666-76.
39. Tsunematsu H, Hifumi H, Kitamura R, Hirai D, Takeuchi M, Ohara M, et al. Analysis of available surface area can predict the long-term dissolution profile of tablets using short-term stability studies. *International journal of pharmaceutics*. 2020;586:119504.
40. Blessy M, Patel RD, Prajapati PN, Agrawal Y. Development of forced degradation and stability indicating studies of drugs—A review. *Journal of pharmaceutical analysis*. 2014;4(3):159-65.
41. Klick S, Muijselaar PG, Waterval J, Eichinger T, Korn C, Gerding TK, et al. Stress testing of drug substances and drug products. *Pharm Technol*. 2005;29(2):48-66.